Thermoelectric properties and electrical characteristics of sputter-deposited p-CuAlO$_2$ thin films

A.N. Banerjee, R. Maity, P.K. Ghosh, K.K. Chattopadhyay*

Department of Physics, Jadavpur University, Kolkata-700 032, India

Abstract

Thermoelectric and electrical properties of transparent p-type CuAlO$_2$ thin films deposited by dc-sputtering method have been studied in detail. Postdeposition annealing in excess oxygen is a necessary precondition of obtaining enhanced p-type conduction in the films. The effect of postdeposition annealing time in excess oxygen on electrical and thermoelectric properties was studied. Thermoelectric measurements of the films, showed considerable high values of room-temperature Seebeck coefficients ranging from 230 to 120 μV K^{-1}, for annealing times of 90 to 30 min, respectively. Natural layered-structure materials, having an effective two-dimensional carrier density, showed an enhanced thermoelectric figure-of-merit. CuAlO$_2$, having a natural superlattice structure, showed very good thermoelectric properties, and it may become a good thermoelectric material for future applications.
© 2004 Elsevier B.V. All rights reserved.

Keywords: CuAlO$_2$; Thermoelectric properties; p-type conductivity; Layered structure; Transparent

1. Introduction

Materials with good thermoelectric properties became part and parcel of the modern technology because of their potential use in cooling systems. Future technology of heat recovery and refrigeration of electronic devices require tailored materials having excellent thermoelectric properties. The commonly used semiconducting thermoelectric materials, such as Bi$_2$Te$_3$ [1], PbTe [2], SiGe alloys [3], etc., are not stable above the 1000 K range and are easily oxidized, whereas for doped FeSi$_2$ [4], although oxidation resistant at and above 1000 K, its thermoelectric properties are still not satisfactory. Thus, attention was generated towards conducting oxides, such as (Zn$_{1-x}$Al$_x$)O [5], (Zn$_{1-y}$Mg$_y$)$_{1-x}$Al$_x$O [6], (Ca$_{1-x}$Bi$_x$)MnO$_3$ [7], CdIn$_{2-x}$Sn$_x$O$_4$, Cd$_2$SnO$_3$, Cd$_2$Sn$_{1-x}$Sb$_x$O$_4$, In$_2$Te$_{1-x}$Re$_x$O$_6$, etc. [8], for possible thermoelectric applications over a wide temperature range.

But their thermoelectric properties are still not up to the mark for superior high temperature performance.

The dimensionless figure of merit ZT [1] provides the measure of the quality of a good thermoelectric material. It is defined as

$$ZT = \frac{S^2 \sigma T}{\kappa} \tag{1}$$

where σ is the electrical conductivity, κ is thermal conductivity and S is the Seebeck coefficient. To achieve high ZT, increase in S and (or) σ and decrease in κ are required. But for simple materials, increase in S leads to a decrease in σ. Similarly, an increase in σ is followed by an increase in κ according to Wiedemann–Franz law. Hence, ZT effectively remains more or less constant. To increase Z, various models have been proposed in the last decade. Amongst them, the most exciting proposal by Hicks et al. [9,10] was superlattice quantum-well materials, having an effective two-dimensional density of states for carriers. This density of state is given by $(m)/(\pi \hbar^2 a)$, where m is the carrier mass and a is the quantum-well width. These authors assumed infinite potential barrier with zero barrier width

---

and showed a considerable increase in Z. Later, Lin-Chung et al. [11] and Broido et al. [12] included the effects of thermal transport in the finite barrier layers and carrier tunneling between layers in the above model to get a modified Z. Encouraged by these findings, various new materials, having layered structure, have been investigated in the last few years, which include $NaCo_2O_4$ [13], $(ZnO)_mIn_2O_3$ [14], $CuAlO_2$ single crystal [15], etc.

Materials of delafossite structure $M^IM^{III}O_2$ (where M^I=Cu, Ag, Pt, Pd; M^{III}=Al, Ga, In, Cr, Fe, Co, etc.) possess natural layered structure [16–18]. Hence, they can become promising thermoelectric materials according to Hicks model. Polycrystalline $CuAlO_2$ thin film is a p-type transparent conducting oxide, which has tremendous potential to be used in optoelectronic device technology [19–21]. In our previous works [22,23], we have reported the synthesis and structural as well as electro-optical characteristics of p-$CuAlO_2$ thin film prepared by dc-sputtering technique. In this communication, we have reported the thermoelectric properties as well as electrical characteristics of this technologically important material. Previously, Koumoto et al. [15] studied the thermoelectric properties of $CuAlO_2$ single crystal and suggested that it may become a good thermoelectric material. From literature survey, it appears that no detail study on the thermoelectric properties of $CuAlO_2$ thin film has been reported so far. In this study, we have prepared the films by dc-sputtering method. During the synthesis process, the postdeposition annealing time (t_a) of the films in O_2 atmosphere was taken as a varying parameter, to observe any variation in the thermoelectric and electrical properties in the films and tried to explain the electrical transport mechanism therefrom. This study may help to produce tailored material having improved thermoelectric and electrical characteristics for better device application.

2. Experimental details

Solid-state reaction between stoichiometric mixture of Cu_2O and Al_2O_3 at 1400 K in air produced $CuAlO_2$ powder. This powder was then placed into a grooved aluminium holder (~5 cm diameter) and pressed into pellet by hydrostatic pressure and used as target for dc sputtering. The sputtering unit was evacuated by standard rotary-diffusion pump arrangement to a base pressure of 10^{-4} Pa. The target was arranged as an upper electrode and -ve bias was applied on it. Ultrasonically cleaned glass and Si substrates were placed on the lower electrode and connected to the ground of the power supply. The electrode distance was taken as 1.8 cm. Ar and O_2 (40 vol.%) were taken as sputtering gas and the sputtering was done in an elevated substrate temperature (~453 K) to achieve high crystallinity in the film. Postdeposition annealing of the films (at 473 K) in an O_2 atmosphere (20 Pa pressure) for different annealing times (t_a) ranging from 30 to 150 min were performed to induce

nonstoichiometry in the films for enhancing p-type conductivity. Details of the deposition conditions were reported elsewhere [22].

The films were characterized by X-ray diffraction (XRD, by CuKα line) to identify the proper phase of the film. Thermoelectric characteristics were measured by copper–constantan thermocouple. Electrical characteristics were measured by standard four-probe method. All contacts were made by silver paste, which showed ohmic characteristics over a wide range of voltages. Thicknesses of the films were estimated from cross-sectional scanning electron microscopy (SEM, JEOL-5200). Compositional analyses of the films were done by energy dispersive X-ray (EDX, Leica S-440, Oxford ISIS) which could detect elements from Boron (5) to Uranium (92).

3. Results and discussion

Three sets of films, prepared at different postdeposition oxygen annealing times (t_a=30, 60 and 90 min), were characterized by X-ray diffraction measurement. Fig. 1 shows the XRD pattern of the $CuAlO_2$ thin film, annealed for 60 min. The substrate was Si (400). The pattern shows a strong (006) orientation. Similar orientations had also been observed previously [19,21]. Other peaks at (003) and (018) have also been observed. This pattern closely reflects the rhombohedral crystal structure with R3m space group [24]. Films deposited at other annealing times (t_a), 30 and 90 min, show identical peaks and are therefore not shown here. This indicates that postdeposition annealing time has no effect on the structural properties of the films. This is probably because, in all three cases, the annealing temperature was kept fixed (at 473 K).

Fig. 2 represents the temperature variation (from 300 to 575 K) of the conductivity (σ) of the films for t_a=30, 60 and 90 min. The thicknesses of the films were around 500 nm, estimated from cross-sectional SEM. An increase in the room-temperature conductivity (σ_{RT}) was observed with the increase in annealing times (t_a). (For example, films with
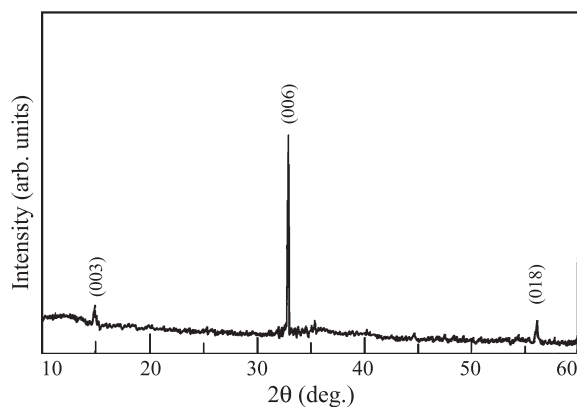

Fig. 1. XRD pattern of $CuAlO_2$ thin film deposited on Si (400) substrate. Annealing time is 60 min and annealing temperature is 473 K.
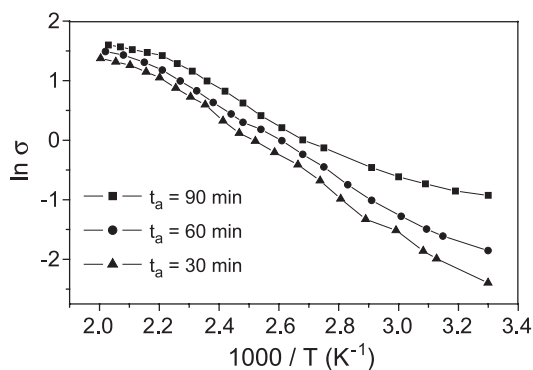
Fig. 2. Temperature dependence of conductivity of $CuAlO_2$ thin films.

t_a=90, 60 and 30 min, σ_{RT}=0.39, 0.16 and 0.09 S cm^{-1}, respectively.) The conductivities range from a minimum of 0.09 S cm^{-1} (for t_a=30 min) to a maximum of 5.0 S cm^{-1} (for t_a=90 min) in the above temperature range. Previously, Kowazoe et al. [19] and Yanagi et al. [21] obtained the room-temperature conductivities for their pulsed laser deposited $CuAlO_2$ thin films on sapphire substrates as 0.095 and 0.34 S cm^{-1}, respectively.

Defect chemistry plays an important role for the increase in p-type conductivity of this material. Metal deficit (or excess oxygen) within the crystallite sites of the material may enhance the p-type conductivity. This deviation from the stoichiometric composition of the components can be induced by regulating the postdeposition annealing time (t_a) in oxygen atmosphere. The approximate defect reaction may be represented by the following equation [15,25]

$$O_2(g) = 2O_O^X + V_{Cu}^- + V_{Al}^{-3} + 4h^+ \qquad (2)$$
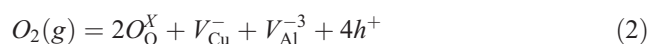
where O_O, V_{Cu}, V_{Al} and h denote lattice oxygen, Cu vacancy, Al vacancy and hole, respectively. Superscripts X, $-$ and $+$ denote effective neutral, negative and positive charge states, respectively. Composition analyses of the films showed that for the unannealed films, the composition is almost stoichiometric. But Hot-probe measurement confirmed the p-type nature of these films. Therefore, it can be argued that some amount of excess oxygen may be present in the unannealed films but the amount is so low that it could not be measured within our experimental limit. This argument seems reasonable if we compare our result with the previously reported values where it has been stated that intercalation of oxygen into the $CuAlO_2$ thin film was not easy [26] and Thomas [20] suggested that the chemical formula of this material would be $CuAlO_{2+x}$ with as low as 0.001 at.% of excess oxygen (i.e., x=1/50,000) over stoichiometric value within the film prepared by Kowazoe et al. [19]. Later, Yanagi et al. [21] performed postdeposition oxygen annealing of the films prepared by the same method as that of Kowazoe et al. [19] and observed a significant increase in the carrier conduction within the films. Although they have not

reported the composition of the films, this enhanced p-type conductivity is most probably due to the presence of excess (nonstoichiometric) oxygen within the film, induced due to postannealing. Similarly, Wang and Gong [27] observed a significant increase in the conductivity of their copper aluminum oxide films after annealing in air. This may be another experimental proof of the suspected p-type conduction caused by excess oxygen. Following this argument, we have performed the postdeposition oxygen annealing of our films to induce excess oxygen within the films for getting enhanced p-type conductivity. We have observed that for the films postannealed for 30, 60 and 90 min, the percentages of excess oxygen were around 0.5, 2.5 and 5 at.%, respectively, over stoichiometric value. The Cu:Al stoichiometry remained close to 1:1 for all the samples. On the other hand, as shown in Fig. 2, an increase in the conductivity with t_a has been observed. Although very little, but still, slight increase in the oxygen content within the films leads to an increase in the conductivity of the films, supporting the above reasoning. But we have seen a decrease in the conductivity when the annealing times were 120 min and above (not shown here). Compositional analyses of the films postannealed for 120 min and above show percentage of excess oxygen within the films more than 10 at.% over stoichiometric value. This suggests that, although the presence of excess oxygen within the films (with t_a=120 min and above) are evidenced, they are not acting favorably to increase the hole conductivity within the films. These excess oxygen atoms most probably lie in the grain-boundary regions as trap states, which put hindrance in the carrier conduction, and hence, a decrease in the conductivity of these films is observed. On the other hand, the films postannealed for 30, 60 and 90 min show an increase in the conductivity along with an increase in the excess oxygen content within the films as mentioned earlier. Therefore, in these cases, the excess oxygen atoms may be acting favorably to generate holes within the films. But it must be admitted that the maximum conductivity obtained for our films was not as much as it would have been. Thus, we suppose that in all cases, whether it is for the films with t_a=90 min or less (when an increase in σ with t_a was observed) or those with t_a=120 min or above (when a decrease in σ with t_a was observed), adsorbed oxygen atoms as trapped states in the grain-boundary regions are always present. In our previous work [22], we have estimated the particle size of our film as 26 nm from XRD data, supported by SEM micrograph. As the particle size is in the nanometer order, a large number of grain boundaries are present in the films; thus, also considerable amounts of trapped states in these grain-boundary regions are present, which put hindrance in the carrier conduction. But for the films with t_a=90 min or less, greater proportion of excess oxygen may be acting favorably towards the hole generation and hence dominate the grain-boundary scat-

tering. This may be the reason for the increase in the conductivity with t_a in this region. On the other hand, for the films with t_a=120 min and above, a greater proportion of the excess oxygen atoms may be adsorbed in the grain-boundary regions, which may probably be correlated with the larger time of exposure of these films in the oxygen atmosphere. Hence, grain-boundary scattering masks the increase in the conductivity and, therefore, we observe a decrease in σ with t_a in this region. But the exact mechanism is still not fully understood.

The activation energies (E_a), which correspond to the minimum energy required to transfer carriers from acceptor level to the valence band (for p-type materials), have been obtained from the slope of the graphs (Fig. 2). The values are 196, 245 and 270 meV for t_a=90, 60 and 30 min, respectively. As expected, the sample with highest conductivity has least E_a value and vice versa. These activation energy values are comparable to the previously obtained values by Kowazoe et al. [19] (200 meV) and Yanagi et al. [21] (220 meV).

Hall effect measurements were done for all three types of samples. All the Hall coefficients were positive, which confirms the p-type nature of the samples. The Hall coefficient (R_H) obtained for the sample with t_a=90 min (σ_{RT}=0.39 S cm^{-1}), is +4.6 cm^3 C^{-1}, corresponding to a hole concentration (n_p) of 1.2×10^{18} cm^{-3}. For the sample with t_a=60 min (σ_{RT}=0.16 S cm^{-1}), these values are +13.9 cm^3 C^{-1} and 4.5×10^{17} cm^{-3}, respectively. And for the sample with t_a=30 min (σ_{RT}=0.09 S cm^{-1}), R_H and n_p are +22.5 cm^3 C^{-1} and 2.8×10^{17} cm^{-3}, respectively. For unannealed films, the Hall measurements could not be performed, but the p-type nature of the films was confirmed by Hot-probe method. Maximum carrier concentration obtained by us is one order of magnitude higher than that reported by Kowazoe et al. [19], but still one order less than that of Yanagi et al. [21]. Further increase in carrier concentration may be done by either regulating the oxygen pressure and (or) substrate temperature during the post-annealing process, or by intentional substitutional doping of the film with appropriate dopant(s), which is the further course of our research work.

Thermoelectric properties of the films were measured from room temperature (300 K) to 550 K. Fig. 3 shows the temperature dependence of Seebeck coefficients (S) for three types of films. All the Seebeck coefficients are positive in nature, which again confirmed p-type conductivity of the films. Room-temperature Seebeck coefficients (S_{RT}) of the films were obtained as 230 μV K^{-1} (for t_a=90 min), 141 μV K^{-1} (for t_a=60 min) and 120 μV K^{-1} (for t_a=30 min). As shown in the figure, the Seebeck coefficients initially decrease from room temperature to around 390 K and then increase to almost 400 μV K^{-1}, for further increase in temperature. Previously, Kowazoe et al. [19] and Yanagi et al. [21] obtained the room-temperature Seebeck coefficients for their pulsed laser deposited CuAlO$_2$ thin film as 183 and 214 μV
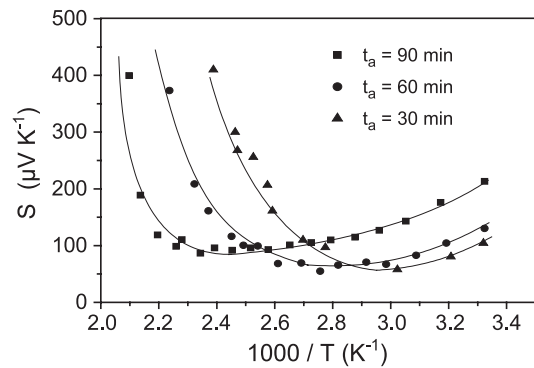

Fig. 3. Seebeck coefficient vs.1000/T of CuAlO$_2$ thin films.

K^{-1}, respectively, which are comparable to our values. On the other hand, Koumoto et al. [15] determined the Seebeck coefficient of CuAlO$_2$ single crystal as well as polycrystal at 600 K around 180 and 150 μV K^{-1}, respectively. In addition, Benko and Koffyberg [28] reported a relatively high value of S_{RT} (670 μV K^{-1}) of CuAlO$_2$ powdered pellets. It has been observed that, in our sputter-deposited CuAlO$_2$ thin film, S_{RT} increases with the increase in conductivity of the films. This observation is consistent with the Hicks model [9,10], where the natural superlattice structure was proposed to show high thermoelectric figure of merit (ZT) due to increase in both S and σ (Eq. (1)). Structure of CuAlO$_2$ delafossite was an alternative stacking of Cu^I and layers of nominal AlO$_2$ composition consisting of Al–O$_6$ octahedra sharing edges. Each Cu atom is linearly coordinated with two oxygen atoms to form a O–Cu–O dumbbell unit placed parallel to the c-axis. O-atoms of O–Cu–O dumbbell link all Cu layers with the AlO$_2$ layers [29]. This structure suggests that CuAlO$_2$ has a layered structure where carriers can easily move two-dimensionally along ab-plane than to move across the Al–O insulating layers. In the XRD pattern (Fig. 1) of our CuAlO$_2$ thin film, we have obtained a strong (006) peak, which is typical of a texture where the c-axis is perpendicular to the substrate (hence parallel to the normal, n to the substrate, i.e., $c \| n$). Now, according to our experimental setup, carriers in the film are expected to move parallel to the substrate, i.e., along the ab-plane; hence, the above argument of two-dimensional confinement of carriers along the ab-plane is valid for our films. Although the reason behind the enhanced thermoelectric properties shown by the materials possessing layered structure is still not fully understood, Koumoto et al. [15] suggested that this may be correlated with the low dimensionality of the crystal structure and the behavior of electrons and phonons in an anisotropic structural environment. Recently, Wang et al. [30] suggested that spin entropy might be responsible for enhanced thermopower in Na$_x$Co$_2$O$_4$ having layered structure [13]. Whether this can be correlated with the good thermoelectric properties of CuAlO$_2$ is still not clear and intense research is needed in this direction.

The variation of thermoelectric power (S) with temperature is given by [31]

$$S = \frac{k}{e}\left(A + \frac{\Delta E_f}{kT}\right) \quad (3)$$

with

$$A = \frac{5}{2} - s \quad (4)$$

and

$$\tau = \tau_o e^{-s} \quad (5)$$

where k is the Boltzmann constant, e is the electronic charge, ΔE_f is the energy difference between Fermi level and the upper edge of the valence band, τ is the relaxation time for electron scattering, s is a constant, which is different for different scattering mechanism and τ_o is a constant, which is a function of temperature but independent of the electronic charge, e.

From Eq. (3), we can obtain the Fermi level (E_f), from the slope of the S vs. $1/T$ graph. From Fig. 3, we determined the Fermi energies for three types of samples from the linear portion of the graphs near room temperature, and the values are 130, 151 and 200 meV for t_a=90, 60 and 30 min, respectively. Previously, Benko and Koffyberg [28] determined the Fermi energy of CuAlO$_2$ powder (σ=1.69×10^{-3} S cm^{-1}) from the thermopower measurement as 190 meV, which is comparable to our sample having lowest room-temperature conductivity (σ_{RT}=0.09 S cm^{-1}, t_a=30 min). As previously mentioned, from the slope of the Ln σ vs. 1000/T plots (Fig. 2), we have obtained the activation energy (E_a) values, which give the estimation of acceptor levels. Comparing these values with the values of Fermi levels, we can say that according to the band picture, Fermi level lies between the upper edge of the valence band and the acceptor level, which is typical of a nondegenerate p-type semiconducting material with acceptors not fully ionized. Hence, a continuous increase in conductivity with temperature was observed for all three types of samples. In addition, it was observed that the sample with maximum conductivity has its Fermi level nearest to the valence band, which is obvious for a p-type material. The values of various electrical and thermoelectric parameters of the thin films are compared in Table 1.

Fig. 4 represents the temperature dependence of thermoelectric power factor (σS^2) of CuAlO$_2$ thin film for the temperature range of 300 to 500 K. The values range from
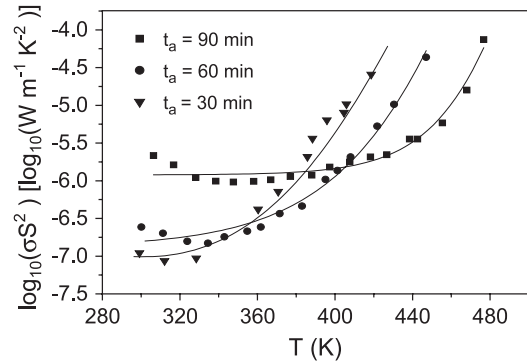

Fig. 4. Thermoelectric power factor vs. temperature of CuAlO$_2$ thin films.

1.1×10^{-7} Wm^{-1} K^{-2} at a temperature around 300 K (for t_a=30 min) to 7.5×10^{-5} Wm^{-1} K^{-2} around 500 K (for t_a=90 min). Koumoto et al. [15] obtained these values roughly as 1.12×10^{-5} Wm^{-1} K^{-2} at 550 K for CuAlO$_2$ single crystal and 7.1×10^{-6} Wm^{-1} K^{-2} at 700 K for CuAlO$_2$ polycrystal. These values are comparable to the values reported by us. This suggests that CuAlO$_2$ thin film could become a good candidate of thermoelectric material, as suggested by Koumoto et al. [15].

4. Conclusions

Thermoelectric and electrical properties of dc-sputter-deposited CuAlO$_2$ thin film has been studied. It appears that, to some extent, postdeposition annealing of the film in oxygen atmosphere controls the p-type conductivity of the film. Compositional analyses reveal an increase in the excess oxygen content within the films with t_a up to 90 min. These values range from 0.5 at.% (for t_a=30 min) to 5.0 at.% (for t_a=90 min) over stoichiometric value, whereas room-temperature conductivities (σ_{RT}) increase from 0.09 to 0.39 S cm^{-1} (for annealing times 30 to 90 min, respectively). This suggests that excess oxygen, within the crystallite sites, may be inducing nonstoichiometry in the film, which, in turn, manifests the improved p-type conductivity of the CuAlO$_2$ thin film. Activation energies range from 270 to 196 meV, respectively. Thermopower measurements indicate that CuAlO$_2$ may become a candidate material for thermoelectric conversion. CuAlO$_2$ has a natural supperlattice structure, with an effective two-dimensional density of states (along ab-plane). This type of layered-structured material could become a good thermoelectric converter.

Table 1
Different thermoelectric and electrical parameters of CuAlO$_2$ thin films, deposited at different annealing times

Sample no.	t_a (min)	σ_{RT} (S cm^{-1})	R_H (cm^3 C^{-1})	n_p (cm^{-3})	S_{RT} (μV K^{-1})	E_a (meV)	E_f (meV)
CAO-42	90	0.39	+4.60	1.2×10^{18}	+230	196	130
CAO-33	60	0.16	+13.9	4.5×10^{17}	+141	245	151
CAO-38	30	0.09	+22.5	2.8×10^{17}	+120	270	200

Room-temperature Seebeck coefficients (S_{RT}) are found to be +230, +141 and +120 μV K^{-1} for t_a=90, 60 and 30 min, respectively, with E_f=130, 151 and 200 meV, respectively. An increase in S_{RT} with σ_{RT} is observed, which is expected for supperlattice materials. In addition, from band picture, it is observed that the higher the conductivity of the film, the closer is its Fermi level to the upper edge of the valence band, which is obvious for a p-type material. Hall measurement study gives the carrier concentration ranging from 1.2×10^{18} to 2.8×10^{17} cm^{-3}. Positive values of Hall and Seebeck coefficients also confirm the p-type nature of the film.

Acknowledgements

References

[1] J.H. Goldsmith, Thermoelectric Refrigeration, Plenum, New York, 1964.
[2] D.M. Rowe, C.M. Bhandari, in: K.R. Rao (Ed.), Proc. 6th Int. Conf. Thermoelec., Arlington, TX, 1986, p. 43.
[3] F.D. Rosi, in: D.D. Allred, C.B. Vining, G.A. Slack (Eds.), Mater. Res. Soc. Symp. Proc., 234, 1991, p. 3, Pittsburgh, PA, 1991.
[4] T. Tokiai, T. Uesugi, K. Koumoto, J. Am. Ceram. Soc. 78 (1995) 1089.
[5] M. Ohtaki, T. Tsubota, K. Eguchi, H. Arai, J. Appl. Phys. 79 (1996) 1816.
[6] T. Tsubota, M. Ohtaki, K. Eguchi, H. Arai, J. Mater. Chem. 8 (1998) 409.
[7] M. Ohtaki, H. Koga, T. Tokunaga, K. Eguchi, H. Arai, J. Solid State Chem. 120 (1996) 105.
[8] R.D. Shannon, J.L. Gilson, R.J. Bouchard, J Phys. Chem. Solids 38 (1977) 877.
[9] L.D. Hicks, M.S. Dresselhaus, Phys. Rev. B 47 (1993) 12727.
[10] L.D. Hicks, T.C. Herman, M.S. Dresselhaus, Appl. Phys. Lett. 63 (1993) 3230.
[11] P.J. Lin-Chung, T.L. Reinecke, Phys. Rev. B 51 (1995) 13244.
[12] D.A. Broido, T.L. Reinecke, Phys. Rev. B 51 (1995) 13797.
[13] I. Terasaki, Y. Sasago, K. Uchinokura, Phys. Rev. B 56 (1997) 12685.
[14] Y. Masuda, M. Ohta, W.S. Seo, W. Pitschke, K. Koumoto, J. Solid State Chem. 79 (2000) 221.
[15] K. Koumoto, H. Koduka, W.S. Seo, J. Mater. Chem. 11 (2001) 251.
[16] R.D. Shannon, D.B. Rogers, C.T. Prewitt, Inorg. Chem. 10 (1971) 713.
[17] C.T. Prewitt, R.D. Shannon, D.B. Rogers, Inorg. Chem. 10 (1971) 719.
[18] D.B. Rogers, R.D. Shannon, C.T. Prewitt, J.L. Gilson, Inorg. Chem. 10 (1971) 723.
[19] H. Kowazoe, M. Yasukawa, H. Hyodo, M. Kurita, H. Yanagi, H. Hosono, Nature 389 (1997) 939.
[20] G. Thomas, Nature 389 (1997) 907.
[21] H. Yanagi, S. Inoue, K. Ueda, H. Kawazoe, H. Hosono, N. Hamada, J. Appl. Phys. 88 (2000) 4159.
[22] A.N. Banerjee, S. Kundoo, K.K. Chattopadhyay, Thin Solid Films 440 (2003) 5.
[23] A.N. Banerjee, R. Maity, K.K. Chattopadhyay, Materials Letters 58 (2003) 10.
[24] Powder Diffraction File, Joint Committee on Powder Diffraction Standards, ASTM, Philadelphia, PA, 1967, Card 9-185.
[25] P. Kofstad, Nonstoichiometry, Diffusion, and Electrical Conductivity in Binary Metal Oxides, Interscience, Wiley, 1972.
[26] R. Nagarajan, A.D. Draeseke, A.W. Sleight, J. Tate, J. Appl. Phys. 89 (2001) 8022.
[27] Y. Wang, H. Gong, Advanced Materials CVD 6 (2000) 285.
[28] F.A. Benko, F.P. Koffyberg, J. Phys. Chem. Solids 45 (1984) 57.
[29] T. Ishiguro, N. Ishizawa, N. Mizutani, M. Kato, J. Solid State Chem. 41 (1982) 132.
[30] Y. Wang, N.S. Rogado, R.J. Cava, N.P. Ong, Nature 423 (2003) 425.
[31] R.K. Willardson, A.C. Beer, Semiconductors and Semimetals, vol. 8, Academic Press, New York and London, 1971.